



Electrical Conductivity Studies of Zinc Oxide, Nickel Doped Zinc Oxide Poly (O-Toluidine) Nanocomposite Using Chemical Oxidative Polymerization



D. Tamilselvi^{1,2*}, N. Velmani³, K. Rathidevi^{4,1}

¹Research & Development Centre, Bharathiar University, Coimbatore – 641 046, Tamilnadu, India

²Department of Science and Humanities, Rathinam Technical Campus, Coimbatore – 641 021, Tamilnadu, India

³Department of Chemistry, Government arts College, Coimbatore -641 018, Tamilnadu, India

⁴Department of Science and Humanities, Kumaraguru College of Technology, Coimbatore – 641 049, Tamilnadu, India

NANOCOMPOSITE semiconductor material comprising Zinc oxide (ZnO), Nickel doped Zinc oxide and Poly(o-toluidine) polymeric composites were synthesized in two stage synthesis process. Solgel technique is adopted in the material synthesis of semiconductor particles of ZnO and Ni/ZnO (NZO), as well a proven technique of chemical oxidation of o-toluidine is attempted to prepare the semiconductor polymeric composites (ZPOT, NZPOT) and pure POT. The synthesized polymeric composites were characterized by (UV-Visible, XRD, SEM, FT-IR and TGA) spectroscopic studies. The addition of semiconductor material into the o-toluidine polymer resulted in a crystalline shape was confirmed from SEM image. Incorporation of metal oxide into polymeric composites showed a significant difference in the conductivity properties which were observed from DC conductivity studies.

Keywords: Poly(o-toluidine), Semiconductor material, Two-stage synthesis, Conductivity studies.

Introduction

Nanoparticles have attracted very much interest in the research field due to their optimized properties and wide range of applications in different areas. The various semiconductors (e.g.: ZnO, TiO₂, WO₃, SnO₂, ZnS, ZnSe, CdS, GaP, GaAs, etc.) are used in different application field Such as optoelectronics, catalysis, solar cells, ultraviolet light emitter, piezoelectric device, chemical gas sensors etc Among these all the semiconductors, ZnO nanoparticle is a nontoxic, low cost and excellent semiconductor nanomaterial with wide band gap of 3.37eV and large excitation binding energy of 60 meV. It is used in electrical, photochemical, catalytic and optoelectronics applications, this can also be used in biomedical applications due to their electrostatic in nature [1-3]. Transition metals

(such as: Ni, CO, Mn, Cr, Fe) doped with ZnO nanomaterials to obtain dilute magnetic semiconductors (DMS). These transition metals improve the electrical, optical and magnetic properties. DMS used in spintronics devices. The doping concentration of the metal with ZnO and calcination process induces some changes in the structure, physical and chemical properties of prepared nanomaterials (ZnO). Some of the dopants, Ni is one of the most favorable transition metals for amalgamate with ZnO, due to their valence, ionic radii are closer to that of Zn²⁺. So Zn²⁺ replaced by Ni²⁺ which gives high donor effect, charge separation and transport in the ZnO nanostructure. Ni doped ZnO nanomaterial is used in several application fields, such as spintronics, photo-electronics devices nano-sensors, nano-generators, metal-ions detection, antifungal activity,... etc [4-10].

*Corresponding author e-mail: tamilselviupdate@gmail.com

Received: 15/07/2019; Accepted: 29/11/2019

DOI: 10.21608/ejchem.2019.14744.1897

©2019 National Information and Documentation Center (NIDOC)

Conducting polymers have created attention over a past decade due to its unique optical and electrical properties which have significant potential commercial applications. Among such conductive polymers polyaniline (PAN) and poly(o-toluidine) (POT) have unusual conductive properties, environmentally stable, ease production, good electrochemical properties and better conductivity [11-13]. Such polymers have wide range of applications in biosensors, rechargeable micro-electronic devices, chemosensors and electrical displays. Polyaniline has provided better conductivity and environmental stability which were its main advantages but, on the contradictory, its insoluble nature in most organic solvents, make it as tough in processing and poly(o-toluidine) fusibility [14-16]. But with the addition of protonic acid substituent in the polyaniline makes it as soluble in organic solvents such as toluene, chloroform, xylene, etc., Hence addition of substituent group into polyaniline makes it as easy to process with better fusibility [10-13]. Poly(o-toluidine)(POT) is the methyl substituted polyaniline conductive polymer which has better solubility nature when compared to polyaniline. Recently PANI doped naphthalene sulphonic acid and camphor sulphonic acid synthesis was reported by the researcher using solid state polymer synthesis method. Polyaniline along with substituents ($-\text{CH}_3$, $-\text{OCH}_3$ and $-\text{OC}_2\text{O}_5$) results in better processability, polymeric network and conductivity nature [17-20].

Polymers with donor atoms have excellent conductivity nature due to the presence of lone pair of electrons present either in the substituent or in the main chain of the polymer skeleton. Polymers with nitrogen atom also play a significant role in the enhanced conductance of the material. Hence amine substituted polymers have good conductance and better stability [21-22].

In this present paper, the aim of this work is to prepare POT, Polymeric composites (ZPOT, NZPOT) by chemical oxidative polymerization in aqueous medium. Addition of dopants such as Zinc oxide (ZnO) and Nickel doped Zinc oxide were synthesized using sol-gel methodology in alkaline medium. Synthesized ZnO, POT and Polymeric composites (ZPOT, NZPOT) were characterized by (UV-Visible, XRD, SEM, FT-IR and TGA) spectroscopic studies. DC conductivity measurements of ZnO, POT and Polymeric composites (ZPOT, NZPOT) were investigated by using four probe DC electrical conductivity

instrument and also compared with that of POT, ZPOT, NZPOT and pure ZnO.

Experimental

Material Required

O-Toluidine ($\text{CH}_3\text{C}_6\text{H}_4\text{NH}_2$, Sigma Aldrich-Germany); Ammonium persulphate ($(\text{NH}_4)_2\text{S}_2\text{O}_8$, Merck, India); Zinc nitrate hexahydrate ($\text{Zn}(\text{NO}_3)_2 \cdot 6\text{H}_2\text{O}$, Merck, India); Sodium hydroxide (NaOH, Himedia, India); Nickel chloride hexahydrate ($\text{NiCl}_2 \cdot 6\text{H}_2\text{O}$, Himedia, India), Hydrochloric acid (HCl, 37%, Loba chemicals, India). Millipore water was purchased and used as such for experiments.

Preparation of zinc oxide (ZnO) and Nickel doped Zinc oxide (NZO)

To prepare pure ZnO, the following steps were involved. 1M of $\text{Zn}(\text{NO}_3)_2 \cdot 6\text{H}_2\text{O}$ was added in 100 ml distilled water in a beaker which forms solution-A. 2M of 100 ml NaOH solution was then added drop-wise to solution-A under vigorous stirring, until an alkaline pH of 12. The stirring action was continued for almost 12 hours. During the preparation of nanoparticles, the solution pH is maintained at 12 because this seems to be the optimum value for the formation of ZnO precipitate. The formed precipitate was then filtered and washed with millipore water and ethanol, dried in oven at 100°C for 2hrs. The dried precipitates were collected and ground in an agate mortar. The same procedure was repeated for another samples preparation. The collected powder samples were then annealed at 500°C for two hours followed by stepwise cooling of 1°C /minute. Similar procedure was followed to prepare Ni-doped ZnO ($\text{Zn}_{0.94}\text{Ni}_{0.06}\text{O}$) using stoichiometric ratios of starting precursors [2-6&30].

Preparation of ZnO-Poly(O-Toluidine) nanocomposites and NZO-Poly(O-Toluidine) nanocomposites.

To prepare pure ZnO-POT nanocomposites via chemical oxidative polymerization method, the following steps were involved. 1.10g of ZnO nanoparticles were dissolved in 10 ml of 1.0 mol/L HCl and the solution was added into 10.63g of o-toluidine monomer was dissolved in 90 ml of 1.0 mol/L HCl and then the mixture was stirred with ultrasonication to accelerate the dispersion. 22.82g of ammonium persulphate (APS) oxidizing agent was dissolved in 100 ml of 1.0 mol/L HCl and the solution was then added drop-wise to the mixture of ZnO nanoparticles

and o-toluidine monomer solution under vigorous stirring in an ice bath for 8–9 hours at 0–5°C. The polymeric solution slowly starts to precipitate out. Finally, the formed precipitated polymer was washed with millipore water and ethanol, until the filtrate was colourless, dried at oven for 12 hours at 60 °C. The final ZnO-POT nanocomposite in base form were received by immersed the above HCl-doped ZnO-POT nanocomposites into 400 ml of 1.0 mol/L $\text{NH}_3 \cdot \text{H}_2\text{O}$ solution under vigorous stirring for 3 hours at room temperature, followed by re-filtered, washed and dried.

The dried dark green precipitates were collected and ground in an agate mortar and stored in desiccator for further use. Similar procedure was followed to prepare NZO-Poly(O-Toluidine) nanocomposites [19-20]. Similar procedure was also followed to prepare pure POT without using of ZnO nanoparticles.

Characterization methods

The functional group present in the polymer and nanocomposites were analyzed using Fourier Transform Infrared Spectrophotometer (FTIR), Shimadzu (Japan) in the range 4000–400 cm^{-1}

with pelletized KBr pellets. The crystalline nature of the semiconductor material, polymer and nanocomposites were characterized using X-Ray Diffraction analyzer (XRD) using X'Pert PRO, X-ray diffractometer with $\text{CuK}\alpha$ radiation ($\lambda=1.5406 \text{ \AA}$). The surface morphology of the samples was analyzed using Scanning Electron Microscope (SEM) with JOEL, JSM and energy dispersive EDX spectrometry. The absorbance and reflectance of the samples were analyzed using UV-reflectance spectra using UV-Vis spectrophotometer model Shimadzu UV-2100. The thermal stability (TGA) of the POT, ZPOT and NZPOT polymeric composites. were analyzed using SDT Q600 V20.9. Electrical conductance of the synthesized ZnO, POT, ZPOT and NZPOT polymeric composites were analyzed using four probe DC electrical conductivity instrument.

Results and Discussion

Fourier Transform Infrared Spectroscopy (FTIR)

The FTIR spectra of ZnO nanoparticles, Ni-ZnO nanoparticles, POT polymer, semiconductor polymeric composites ZPOT and NZPOT were presented in Fig. 1.

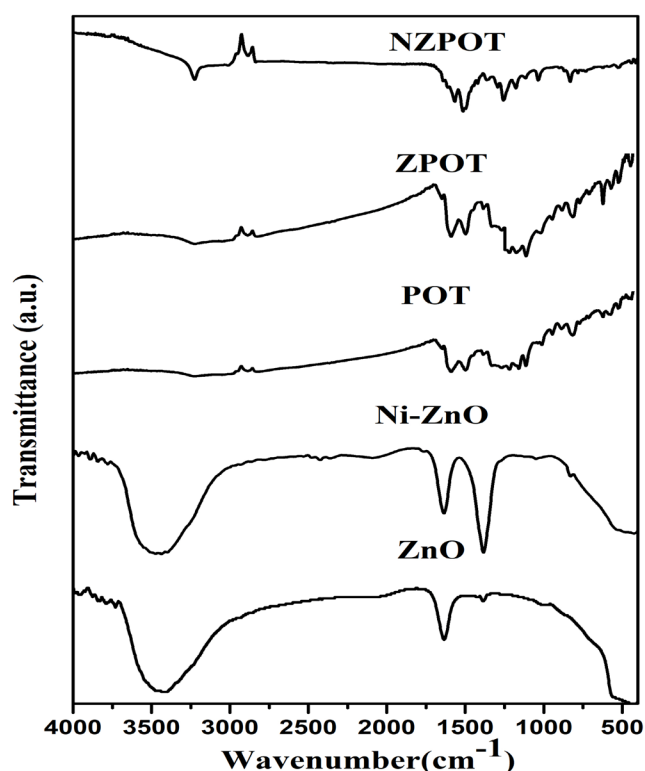


Fig. 1. FTIR spectra of ZnO, Ni-ZnO, Poly(o-toluidine) (POT); Zinc-POT polymeric composites (ZPOT) and Nickel doped Zinc oxide POT polymeric composites (NZPOT).

The formation of ZnO nanoparticle showed a peak at 3442 cm^{-1} and 1634 cm^{-1} corresponding to O-H stretching and bending vibrations of water molecules and the peaks at 1383 cm^{-1} corresponding to the presence of NO_3^- was confirmed. A peak around 432 cm^{-1} corresponding to the formation of Zn-O metal oxide bond [29]. The formation of Ni-ZnO nanoparticle showed peaks at 3461 cm^{-1} and 1633 cm^{-1} corresponding to O-H stretching and bending vibrations of water molecules and the peaks at 1383 cm^{-1} corresponding to the presence of NO_3^- was confirmed. A peak around 403 cm^{-1} corresponding to the formation of Zn-O metal oxide bond [(3-6]. The formation of POT polymer showed a peak at 2910 cm^{-1} corresponding to the C-H stretching of the methyl group. The peaks at 1590 cm^{-1} and 1494 cm^{-1} corresponding to C=C stretching vibration of quinoid and benzenoid rings in POT polymeric chain. The peaks at 1379 cm^{-1} and 3213 cm^{-1} corresponding to C-N and N-H stretching vibration linked to benzenoid rings in POT polymeric chain. The peaks at 1155 cm^{-1} and 810 cm^{-1} corresponding to C-H plane stretching vibration of quinoid rings and C-H out plane bending vibration of benzenoid rings. The formation of ZnO/POT(ZPOT) polymeric nanocomposites showed an absorption peaks are centered at around $3203, 2799, 1588, 1485, 1214, 1107$ and 809 cm^{-1} respectively. The formation of Ni-ZnO/POT (NZPOT) polymeric nanocomposites showed an absorption peaks are centered at around $3221, 2787, 1563, 1417, 1251, 1030$ and 779 cm^{-1} respectively [23].

Comparing to that of pure POT polymer, the absorption peaks of ZnO/POT(ZPOT) and Ni-ZnO/POT (NZPOT) polymeric nanocomposites have been shifted to lower wave numbers, the shift of absorption peaks may be corresponding to the formation of hydrogen bonding between nano ZnO and the -NH group of POT polymer on the surface of the ZnO nanoparticles. In case of Zn-O nanoparticles a peak at around 432 cm^{-1} corresponding to Zn-O stretching was observed, but found to be weak in ZnO/POT(ZPOT) and Ni-ZnO/POT (NZPOT) polymeric nanocomposites because of the presence of interactions between POT and ZnO/Ni-ZnO nanoparticles. These results suggest that ZnO/Ni-ZnO nanoparticles were effectively covered by POT [20-23]. The main reason for the incorporation of the semiconductor material into the polymeric lattice is to improve the conductivity and thereby increasing the free flow of electrons in the polymeric chain. The

secondary amine present in the polymeric chain also plays a significant role in the conductivity due to the presence of lone pair of electrons present on the polymeric backbone.

The XRD patterns of ZnO nanoparticles, POT polymer, and NZPOT polymeric composites were presented in Fig. 2. From the observed results, it was clear that the POT polymer shows a single broad peak at 2θ values around 25° , which indicates POT polymer has an amorphous structure (or) semi crystalline, since there were no sharp peaks were integral factor occurred in the XRD image [23&27]. But when the XRD image of ZnO semiconductor material was noted, it was observed that there were sharp peaks corresponding to the formation of hexagonal wurtzite structure. The peak reflections at theta values $31.81^\circ, 34.44^\circ, 36.31^\circ, 47.602^\circ, 56.62^\circ, 63.01^\circ, 66.48^\circ, 67.97^\circ,$ and 69.19° corresponds to the (100), (002), (101), (102), (110), (103), (200), (112), and (201) planes which was in agreement with JCPDS no. 36-14 [2-5&29]. When the semiconductor material was mixed with the poly(o-toluidine), the crystalline nature diminished due to the minimal amount of semiconductor added during the synthesis of semiconductor polymeric composites which resulted in a crystalline nature. This was observed with the considerable change in the XRD image of the polymeric composites. These XRD results justified the incorporation of semiconductor material into the polymeric chain would result in enhanced conductivity [18-19].

UV-Vis spectral studies

The optical properties of the POT polymer, Zinc oxide (ZnO), the semiconductor polymeric composites, ZPOT and NZPOT were analyzed using UV-Visible spectral studies and the result was shown in Fig. 3 (a). The UV spectra showed 3 predominant peaks at $320\text{ nm}, 440\text{ nm}$ and 845 nm respectively. The peak at 320 nm corresponded to the $\pi-\pi^*$ transition of the benzenoid rings. The localized polarons characterized protonated poly(o-toluidine) showed a peak at 40 nm . The peak at 845 nm attributed to the emeraldine form of conducting POT polymer. An absorption band observed around 369 nm corresponds to the agglomeration of ZnO and Ni- ZnO nanoparticles. Apart from that, an absorption band at 260 nm represents the ZnO nanoparticles of wavelength below 3.65 eV . With the incorporation of Zinc oxide POT conducting polymer composites (ZPOT) and Nickel doped Zinc oxide POT polymer composites (NZPOT) showed no significant difference in the

optical spectra exhibited with the UV-Vis spectra. These results proved that the optical properties of the parent POT polymer do not change even after the addition of dopant which showed no change in the carbon skeleton of the polymeric backbone chain [20-22].

The optical band gap E_g was obtained by the modified Kubelka-Munk (K-M) function $[F(R) / hv]^2$ versus photon energy (eV) $[F(R) / hv]^2 = \{(1-R)^2/2R\} * hv^2$ and the result was shown in Fig. 3(b). The optical band gap value of the ZnO, Ni-ZnO, POT, ZPOT and NZPOT samples exhibited as 3.27 eV for sample (a), 3.18 eV for sample (b), 2.40 eV for sample (c), 2.39 eV for sample (d) and 2.37 eV for sample (e) respectively [6,27&28].

Scanning Electron Microscope (SEM) studies

The surface morphological nature of the POT polymer, ZPOT and NZPOT polymeric composites were analysed using SEM studies and presented in the Fig 4(A-E). Figure 4(A) shows

that amorphous (or) semi crystalline structure of POT formed with irregular agglomerations, which connected with each other and the structure with few small pores. The SEM image of Zinc oxide POT polymeric composites was shown in Fig.4(B). Incorporation of Zinc oxide into POT polymer shows that hexagonal shaped crystalline nature, when compared with pure POT polymer, the hexagonal crystal structure was observed signifying the formation of Zinc oxide. The Nickel doped zinc oxide POT polymer composites were shown in Fig. 4(C). In this SEM image, hexagonal structured shaped particles diminished with the formation of convulsions due to the addition of dopant Nickel doped Zinc oxide. The SEM image of ZnO was shown in Fig. 4(D). Non-uniform irregular shaped nanoparticle was observed with average size of ZnO nanoparticle was of 96 to 110 nm respectively. The SEM image of Ni-ZnO was shown in Fig. 4(E) from this hexagonal crystal structure was observed.

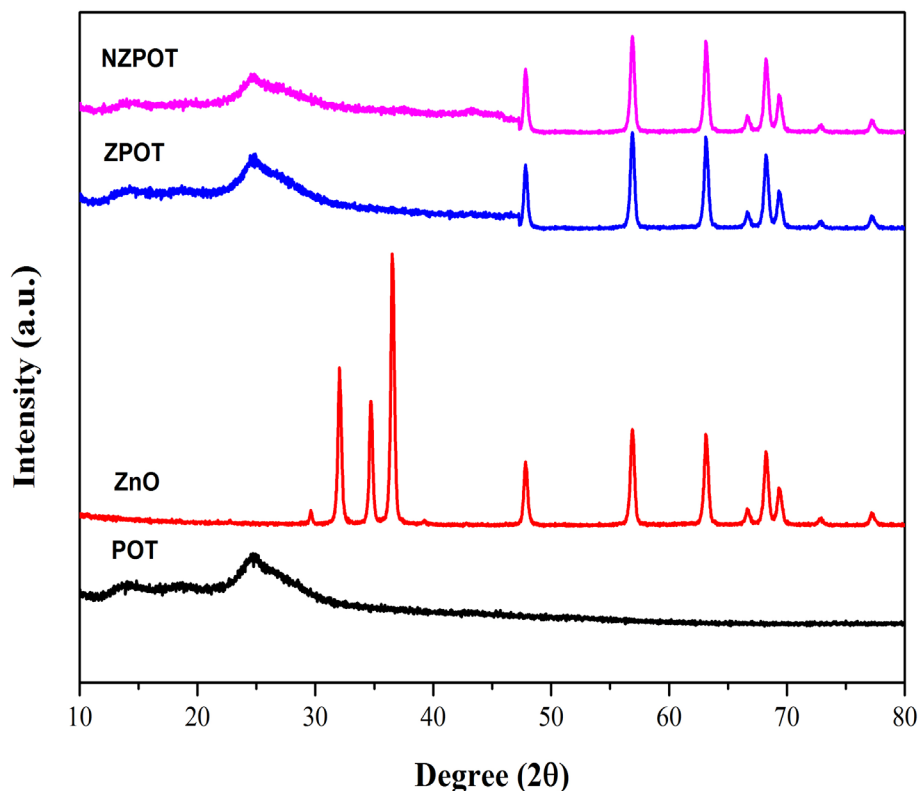


Fig. 2. XRD analysis of ZnO, Poly(o-toluidine) (POT); Zinc-POT polymeric composites (ZPOT) and Nickel doped Zinc oxide POT polymeric composites (NZPOT).

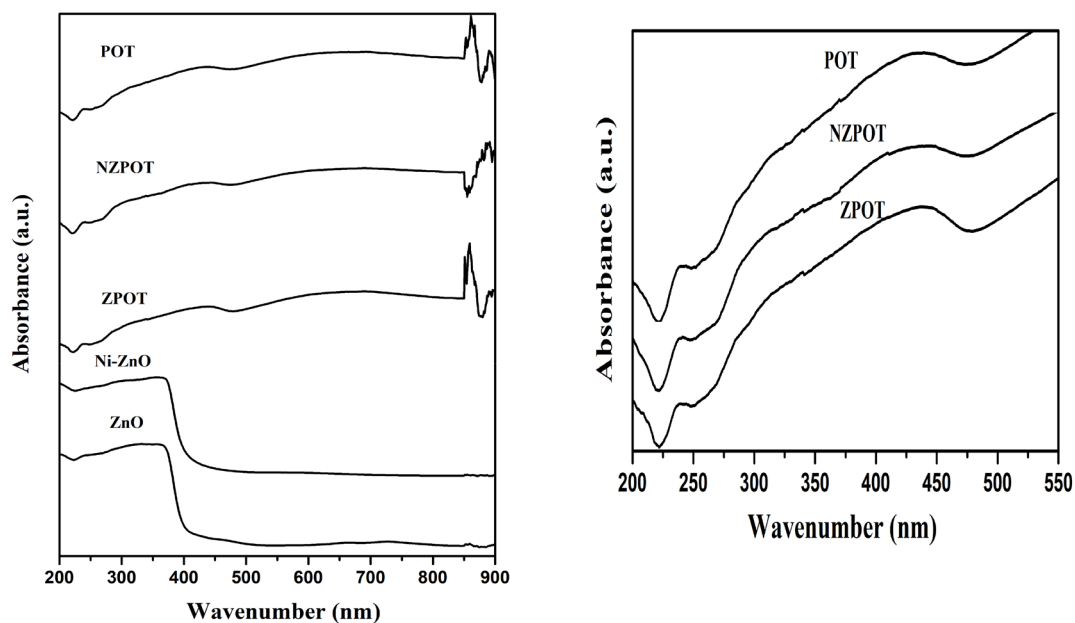


Fig. 3 (a). UV-Vis spectra of ZnO, Ni-ZnO, Poly(o-toluidine) (POT); Zinc-POT polymeric composites (ZPOT) and Nickel doped Zinc oxide POT polymeric composites (NZPOT).

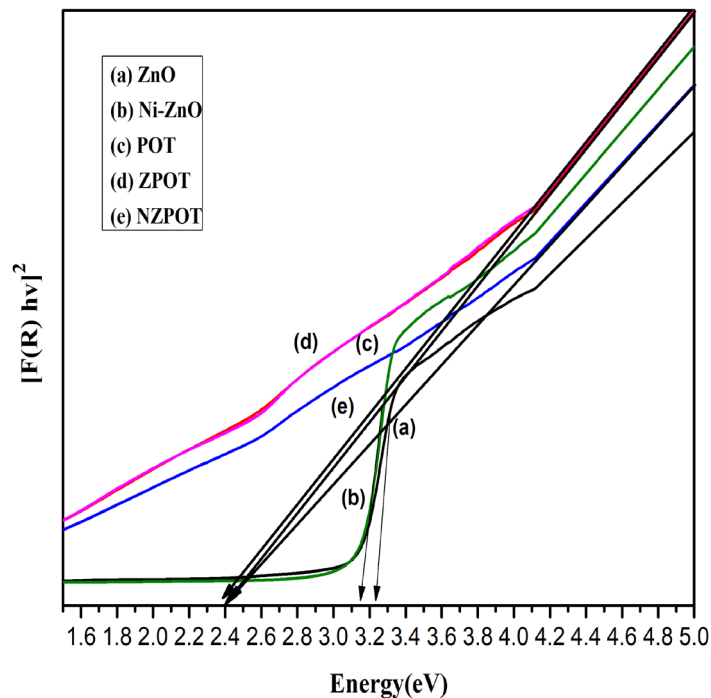


Fig. 3 (b). Band gap graph of ZnO, Ni-ZnO, POT, ZPOT & NZPOT.

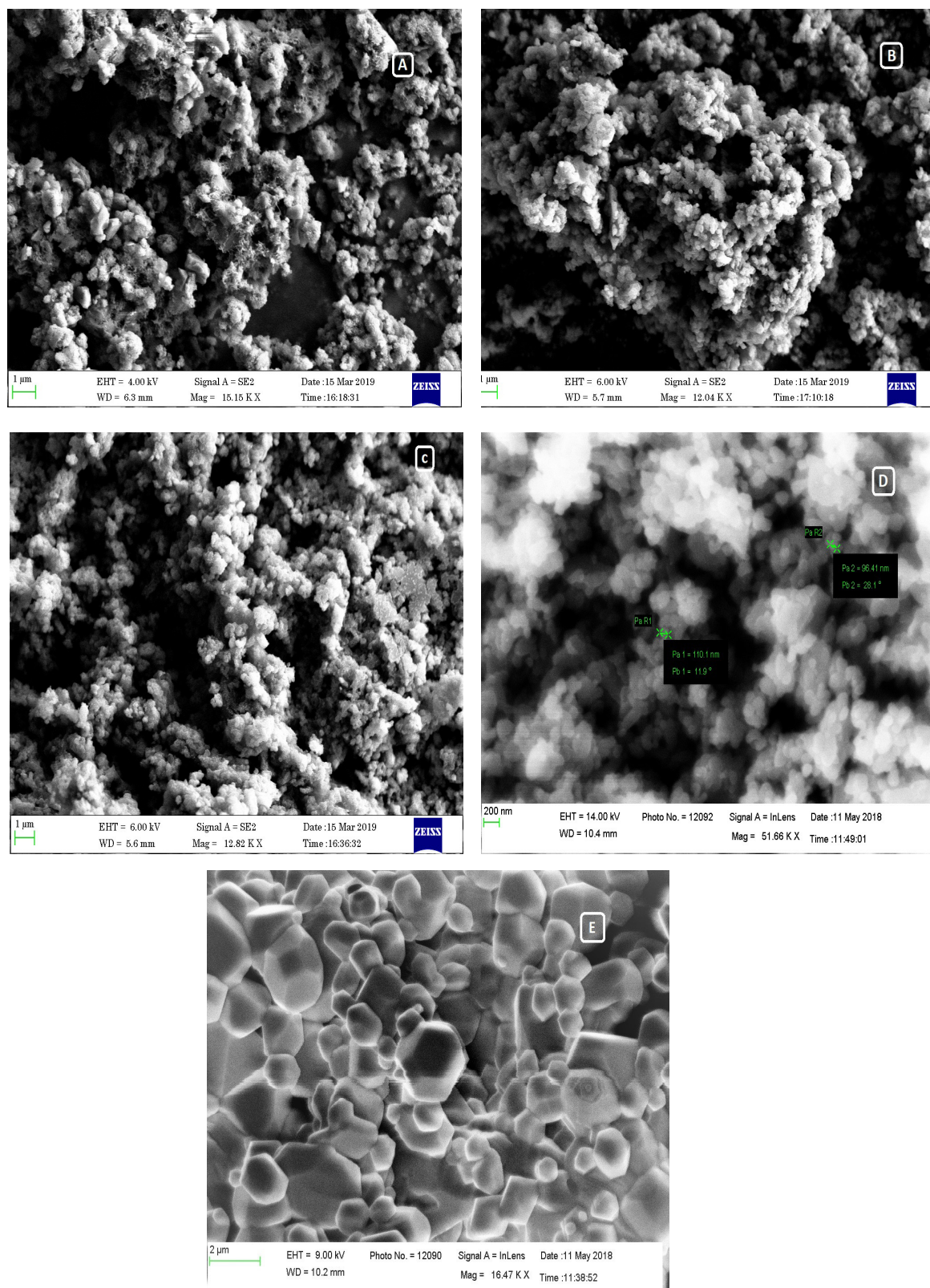


Fig. 4 (A-E). SEM images of ZnO, Ni-ZnO, Poly(o-toluidine) (POT); Zinc-POT polymeric composites (ZPOT) and Nickel doped Zinc oxide POT polymeric composites (NZPOT). 4(A). SEM image of POT polymer; 4(B). SEM image of ZPOT polymer composites; 4(C). SEM image of NZPOT polymer composites; 4(D)& 4(E). SEM image of Ni-ZnO nanoparticles.

Thermogravimetric analysis of POT, ZPOT and NZPOT polymeric composites

The thermal profile of the POT polymer, ZPOT and NZPOT polymeric composites were presented in Fig. 5. When the thermal profiles of synthesized polymeric materials were compared there exist only finite differences in the reducing of weight loss with respect to temperature range from 25 to 900°C. There was no much difference in the thermal profile. A three-stage thermal decomposition takes place for all three synthesized polymeric materials. In the first stage there was about 5% weight loss from 25 to 110°C, which is attributed due to the removal of free water molecules from polymer matrix, In the second stage start from 110°C to about 400 °C there is a 4-5% of weight loss by virtue of eliminating the dopant ions as well as bound water from polymer chains and the third stage start from 400 °C onwards polymer starts to degradation, due to the thermal degradation and decomposition of the skeletal backbone of the polymeric chain along with the loss of the dopant. The final stage of decomposition starts from above 500 °C, weight loss is mainly due to the complete degradation of the substituent present in the benzene ring of the polymeric backbone. The presence of substituent group in the ortho position of the polymeric backbone and steric effect results in the loosening of the polymeric matrix requires

only small energy for the complete breakdown of the polymer chain [15]. The weight loss percentage of POT is 61.43% at 900°C, while the weight loss percentage of ZPOT is 49.20 % and while the weight loss percentage of NZPOT is 45.54 %.

Electrical conductivity

The conductivity studies of ZnO, Poly(o-toluidine) conducting polymer (POT), Zinc oxide doped POT polymeric composites (ZPOT) and Nickel doped zinc oxide POT polymeric composites (NZPOT) conducting polymeric composites against difference in temperature is presented in Figure 6. Conductivity was measured by using Ohm's law, $V = RI$ where, I is the current (in Amperes) through a resistor R (in ohms) and V is the drop-in potential (in volts) across it. The reciprocal of resistance (R^{-1}) is called conductance, the flow of current I as a result of gradient in potential leads to energy being dissipated (RI^2 joule s^{-1}). In Ohmic material, the resistivity measured is proportional to the sample cross-section A and inversely proportional to its length l : $R = \rho l / A$ where ρ is the resistivity measured in Ω cm. Its inverse $\sigma = \rho^{-1}$ is the conductivity. It was found that Dc conductivity of ZnO, POT polymer, ZPOT and NZPOT samples were shown in Table 1.

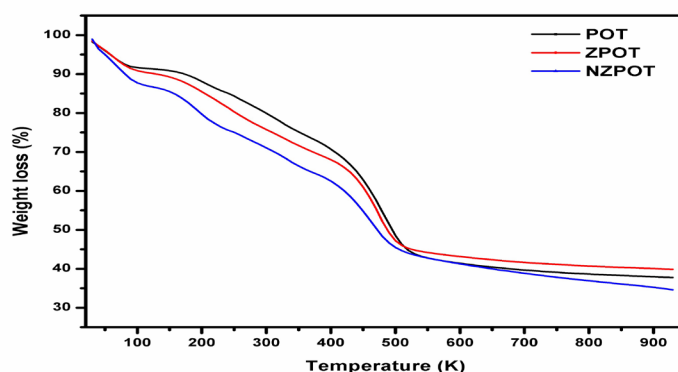


Fig. 5. Thermal profile of POT polymer, ZPOT and NZPOT polymeric composite.

TABLE 1. DC Conductivity of ZnO, POT polymer, ZPOT and NZPOT samples.

TEMP(K)	\ln of $\sigma = 1/\rho$ (20mA)			
	ZnO	POT	ZPOT	NZPOT
307	6.930131	7.064791	7.494749	8.347552682
313	6.936717	7.074628	7.497355	8.357132919
333	6.972538	7.078427	7.516943	8.373818511
353	6.985125	7.097741	7.518983	8.395641527
373	6.993430	7.105679	7.525584	8.411170621
393	7.022165	7.115645	7.529120	8.437391315
413	7.042515	7.127062	7.533146	8.458390807
433	7.081761	7.129124	7.537156	8.469479630

A steady and gradual increase in electrical conductance for ZnO, POT, ZPOT and NZPOT synthesized polymeric materials prevails with increase in temperature (K). Conductivity slowly increases for all four conducting polymeric materials with increase in temperature. As a result, the conductance of the Nickel doped zinc oxide poly(o-toluidine) (NZPOT) polymeric composites showed enhanced electrical conductance compared to ZnO nanoparticle, ZPOT polymeric composite and POT conducting polymer, due to the addition of nickel doped zinc ion into the polymeric lattice resulted in the enhanced conductivity. This steady increase in the electrical conductance was due to presence of lone pair of electrons present in the secondary amine of the polymeric backbone and the electropositive dopants atoms. These electrons will flow freely along the band edge position thus resulting in the gradual increase in the electrical conductance [24&29]. This was evident from Fig. 6.

The Arrhenius plot of dc conductivity against difference in temperature was shown in Fig. 7. The activation energies for two regions were measured with the operating mechanism of trapped or scattering ions. With addition of dopant from single and multi-component dopant system, the activation energy raises which accounts for the electrical conductance and the atomic defect of the polymeric composites system. Thermal excitation from donor levels to the conduction band from the valence level takes place with the incorporation of dopant into the polymeric backbone. The donor carrier density decreases with increase in the activation energy, as a result the electrons to move from valence band to conduction band easily causing increased flow of conductance for doped polymeric composites when compared with the pure conducting polymer.

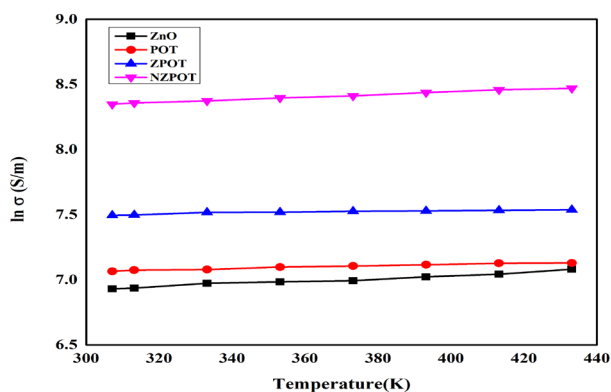


Fig. 6. Electrical conductance of the synthesized polymeric material against temperature (K),

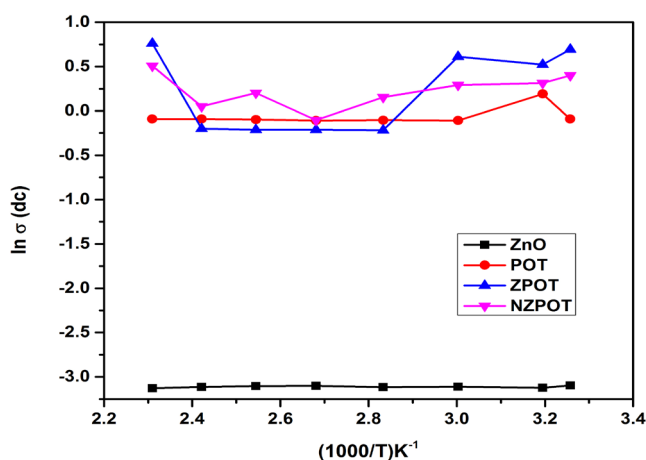


Fig. 7. Arrhenius plot of conductivity of synthesized polymeric material against temperature difference.

Conclusion

Zinc oxide and Nickel doped Zinc oxide were synthesized using sol-gel methodology in alkaline medium. Poly(o-toluidine) (POT) conducting polymer, Zinc oxide doped POT polymeric composites and nickel doped zinc oxide POT polymeric composites were synthesized using one-pot oxidative polymerization reaction using ammonium persulphate (APS) reagent. The spectral characterization results justified the formation of the polymers and polymeric composites. The XRD images confirmed the formation of Zinc oxide with sharp peaks and addition of POT polymer resulted in the broad peaks. The UV studies showed a peak at 440 nm corresponding to the substituted poly(o-toluidine). The peak at 845 nm attributed to the emeraldine form of conducting POT polymer. Upon comparison, the electrical conductance of the nickel doped POT polymeric composites showed enhanced electrical conductance with increase in temperature was observed, due to the presence of dopant along with the lone pair of electrons present in the polymeric backbone.

References

- Hasnidawani J.N., Azlina H.N., Norita H., Bonnia N.N., Ratim S. and Ali E.S., Synthesis of ZnO Nanostructures Using Sol-Gel Method, *Procedia chemistry*, **19**, 211-216 (2016).
- Venu Gopal V.R., Susmita Kamila, Effect of temperature on the morphology of ZnO nanoparticles a comparative study, *Appl Nanosci*, **7**, 75-82 (2017).
- Debadrito Das, Animesh kumar Datta, Divya Vishambhar Kumbhakar, Bapi Ghosh, Ankita Pramanik, Sutha Gupta, Conditional optimization of wet chemical synthesis for pioneered ZnO nanostructures, *Nano-Structures & Nano-Objects*, **9**, 26-30 (2017).
- Zafaran Abdul Fattah et al., Synthesis and characterization of Nickel doped Zinc Oxide Nanoparticles by Sol-gel method, *International Journal of Engineering Sciences & Research Technology*, **5** (7) (2016).
- Yuanyou Wang, Tianqing Liu, Qingli Huang and Changle Wu, Dan Shan, Synthesis and their photocatalytic properties of Ni-doped ZnO hollow microspheres, *J. Mater. Res.*, Vol. 31, No. **15**, (2016).
- Fabbiyola S., Sailaja V., John Kennedy L., Bououdina M., Judith Vijaya J., Optical and Magnetic properties of Ni-doped ZnO nanoparticles, *Journal of Alloys and Compounds*, **694**, 522- 531, (2017).
- Umadevi Godavarti, Mote V.D., Madhavaprasad Dasari, Precipitated nickel doped ZnO nanoparticles with enhanced low temperature ethanol sensing properties, *Modern Electronic Materials*, **3**, 179-185 (2017).
- Gadalla A.A., Israa Abood, Elokr M.M., Structural, Optical and Magnetic Properties of Ni-doped ZnO Synthesized by Co-precipitation method, *Journal of Nanotechnology and Materials Science*, **4** (1), 19-26 (2017).
- Sankar Ganesh R., Durgadevi E., Navaneethan M., Patil V.L., Ponnusamy S., Muthamizhchelvan .C, Kawasaki.S, Patil.P. S, Hayakawa.Y, Controlled synthesis of Ni-doped ZnO hexagonal microdiscs and their gas sensing properties at low temperature, *Chemical Physics Letters*, **689**, 92-99 (2017).
- Anindita Samanta, Goswami M.N., Mahapatra P.K., Magnetic and electric properties of Ni-doped ZnO nanoparticles exhibit diluted magnetic semiconductor in nature, *Journal of alloys and compounds*, **730**, 399-407 (2018).
- Poyraz S., Liu Z., Liu Y., Lu N., Kim M.J., Zhang X.Y., One-step synthesis and characterization of poly(o-toluidine) nanofiber/metal nanoparticle composite networks as non-enzymatic glucose sensors, *Sens. Actuators B*, **201**, 65– 74 (2014).
- Shama Islam, Mohsin Ganaie, Shabir Ahmad, Siddiqui Azher M. and Zulfequar M., Dopant Effect and Characterization of Poly (O-Toluidine)/ Vanadium Pentoxide Composites Prepared by in Situ Polymerization Process, *International Journal of Physics and Astronomy*, Vol. 2, No. 2, pp. 105-122 (2014).
- Shakir M., Khan M. S., Al-Resayes S. I., Baig U., Alam P., Khan R. H. and Alam M., In-vitro DNA binding, molecular docking and antimicrobial studies on newly synthesized poly(o-toluidine)-titanium dioxide nanocomposite, *Royal Society of Chemistry Adv.* (2014).
- Mohammed Kashif Sharif Ahmad, Poly ortho toluidine dispersed castor oil Polyurethane anti corrosive nanocomposite coatings, *Royal Society of Chemistry Adv.*, **4**, 20984 (2014).

15. Salma Bilala, Shehna Farooqa, Anwar-ul-Haq Ali Shahb, Rudolf Holzec, Improved solubility, conductivity, thermal stability and corrosion protection properties of poly(o-toluidine) synthesized via chemical polymerization, *Synthetic Metals*, **197**, 144–153 (2014).
16. Asif Ali Khan and Shakeeba Shaheen, Electrical conductivity, isothermal stability and amine sensing studies of a synthetic poly o-toluidine/multiwalled carbon nanotube/Sn(IV)tungstate composite ion exchanger doped with p-toluene sulfonic acid, *Royal Society of Chemistry Adv.*, **7**, 2077 (2015).
17. Liu J., Wen, Z.P. Liu X.H., Tan Y., Yang S.Y., Zhang P., Electrorheological performances of poly(o-toluidine) and p-toluenesulfonic acid doped poly(o-toluidine) suspensions, *Colloid. Polym. Sci.*, **293**, 1391–1400 (2015).
18. Fakher Alfahed R. K., Ajeel K. I., Effect of Cobalt's Chloride on the Electrical Properties of Poly (O-Toluidine), *International Journal of Materials Science and Engineering*, Volume 3, **4**, (2015).
19. Jiwei Huang Chuanbo Hu Yongquan Qing, Preparation and Corrosion Resistance of poly(o-toluidine)/nano SiC/epoxy Composite Coating, *Int. J. Electrochem. Sci.*, **10**, 10607 – 10618 (2015).
20. Chuanbo Hu, Ying Li, Yazhou Kong, Yushi Ding, Preparation of poly(o-toluidine)/nano ZnO/epoxy composite coating and evaluation of its corrosion resistance properties. *Synthetic Metals*, **214**, 62–70 (2016).
21. Hajera Gul Salma Gul, Anwar-ul-Haq Ali Shah & Salma Bilal, Poly(o-toluidine) salt as low cost electrode material for high performance electrochemical supercapacitor, *Indian journal of chemistry*, Vol. **56A**, pp. 493-500, May (2017).
22. Hesampour.M., Taher M. A. and Behzadi M., Synthesis, characterization and application of MnFe₂O₄@poly(o-toluidine) nanocomposite for magnetic solid-phase extraction of polycyclic aromatic hydrocarbons, *New Journal of Chemistry*, (2017).
23. Shama Islam, Hana Khan, Zubair MSH Khan, Shabir Ahmad Kumar, Raja Saifu Rahman and M. Zulfequara, Novel Approach to Synthesis and Characterization of POT/ZnO nanocomposites, *American Institute of Physics*, **1953**, 130028 (2018).
24. Seema joon, Rakesh kumar, Avanish Pratap Singh, Rajni Shukla and Dhawan S.K., Lightweight and solution processible thin sheets of Poly-(O-Toluidine)-Carbon fiber-novolac composite for EMI shielding, *Royal Society of Chemistry Adv.*, **5**, 55059 (2015).
25. Sandeep Kaushal, Rahul Badru, Sanjeev Kumar, Susheel K. Mittal and Pritpal Singh, Fabrication of mercury (II) ion selective electrode based on Poly O-Toluidine-Zirconium phosphoborate, *Royal Society of Chemistry Adv.*, **6**, 3150 (2016).
26. Kiran Kumari, Vazid Ali, Gita Rani, Sushil Kumar, Lakshmi G. B. V. S., Zulfequar M., DC Conductivity and spectroscopic Characterization of Poly(O-Toluidine) doped with binary dopant ZrOCl₂/Ag/I, *Materials Sciences and Application*, **2**, 1049-1057 (2011).
27. Anand Kumar, Vazid Ali, Sushil Kumar & Husain M., Studies on conductivity and optical properties of Poly(O-Toluidine)-Ferrous sulfate composites, *International Journal of Polymer Analysis and Characterization*, **16**, 298-306 (2011).
28. Umadevi Godavarti, Mote V.D., Madhavaprasad Dasari, Role of cobalt doping on the electrical conductivity of ZnO nanoparticles, *Journal of Asian Ceramic Societies*, **5**, 391-396 (2017).
29. Morsi S.M.M., Mohsen R.M., Selim M.M., El-Sherif H.S., Sol-gel, Hydrothermal, and Combustion Synthetic Methods of Zinc Oxide Nanoparticles and Their Modification with Polyaniline for Antimicrobial Nanocomposites Application, *Egyptian Journal of Chemistry*, Vol. **62**, No. 6. pp. 1531 - 1544 (2019).
30. Aparna Mohan, Nimisha K.V., Janardanan.C., Removal of chlorobenzene and 1,4-dichlorobenzene using novel poly-o-toluidine zirconium (IV) phosphotellurite exchanger, *Resource-Efficient Technologies*, **3**, 317-328, (2017).
31. Hussam Musleh, Hamdia Zayed, Samy Shaat, Amal Al-Kahlout, Hassan Tamous, Ahmed Issa, Jehad Asad and Naji AlDahoudi, Enhancement of The Performance of Dye-sensitized Solar Cells Using Sensitized Zinc Oxide Nanoparticles by Rhodamine B dye, *Egyptian Journal of Chemistry*, The First International Conference on Molecular Modeling and Spectroscopy pp. 111-123 (2019).